Comparison on process efficiency for CLC of syngas operated in packed bed and fluidized bed reactors

H.P. Hamers [a], M.C. Romano [b], V. Spallina [a], P. Chiesa [b,*], F. Gallucci [a], M. van Sint Annaland [a]

[a] *Chemical Process Intensification, Department of Chemical Engineering and Chemistry, Eindhoven University of Technology, P.O. Box 513, 5600MB Eindhoven, The Netherlands*
[b] *Group of Energy Conversion Systems, Department of Energy, Politecnico di Milano, Via Lambruschini 4, 20156 Milano, Italy*

Received 22 February 2014
Received in revised form 7 June 2014
Accepted 9 June 2014

1. Introduction

It is widely accepted and recently confirmed that climate change is occurring and is likely to be caused by anthropogenic CO_2 emissions (IPCC, 2013). Therefore, methods to reduce these emissions have been studied for several years. A possible solution to decrease the CO_2 emissions is equipping fossil fuel-fired power plants with CO_2 capture processes for long term storage. A large disadvantage of implementing carbon capture and storage (CCS) in power plants is that quite some energy is consumed by the CO_2 capture step and therefore the overall process efficiency decreases. This process efficiency drop might be reduced by implementing advanced technologies like chemical-looping combustion (CLC), a process where the CO_2 capture is integrated with the power production process. The integration of reaction and separation is reached by oxidizing the fuel without direct contact with air (thus circumventing the mixing of nitrogen and CO_2); instead, a metal oxide behaving as oxygen carrier is used to transport the oxygen from the air reactor

* Corresponding author. Tel.: +39 0223993916.
E-mail address: paolo.chiesa@polimi.it (P. Chiesa).

Nomenclature

Abbreviations

ASU	air separation unit
BOP	balance of plant
CCS	carbon capture and storage
CLC	chemical-looping combustion
CGD	cold gas desulfurization
EBTF	European Benchmarking Task Force
eco	economizer
eva	evaporator
FzB	fluidized bed configuration
GS	gas–steam cycles software
GT	gas turbine
HGD	hot gas desulfurizaton
HP	high pressure
HRSC	heat recovery steam cycle
HRSG	heat recovery steam generator
L/*D*-ratio	length/diameter ratio
LHV	low heating value (J/mol)
PB	packed beds configuration
SH	super heater
SPECCA	specific primary energy consumptions for CO_2 avoided, MJ_{LHV}/kg_{CO_2}
ST	steam turbine
TIT	turbine inlet temperature
TSA	temperature swing adsorption
WGS	water gas shift reaction

Symbols

C	costs of component, €
D	inner diameter of reactor, m
D_a	inner reactor and refractory diameter, m
d_p	particle diameter, m
E_{CO_2}	specific CO_2 emissions, kg/MWh_e
f	design stress of carbon steel, Pa
L	reactor length, m
N_R	number of reactors, –
$\dot{m}$	total mass flow that is processed during an operation step, kg/s
$\dot{m}$	molar flow, kmol/s
P_{in}	pressure of the vessel, Pa
Q	heat losses, W
s	thickness
$T_{max,\,CLC}$	temperature inside reactor, K
T_{steel}	temperature of the steel vessel, K
V	volume flow rate, m^3/s
V_R	volume of reactor, m^3
v_g	superficial velocity, m/s

Greek

ΔX_s	conversion of the oxygen carrier, –
ε_g	void fraction, $m^3_{gas}/m^3_{reactor}$
η	net electric efficiency, –
η_g	dynamic gas viscosity, kg/(m s)
λ	thermal conductivity, W/(m K)
ρ_g	gas density, kg/m^3
$\rho_{mol,oxygen}$	amount of atomic oxygen per m^3 of reactor, $kmol/m^3$
τ	cycle time, s
φ_{step}	the portion of reactors operating under the considered step

Subscript

e	electrical
in	inner
r	refractory
ref	reference plant without CO_2 capture
th	thermal
wall	reactor vessel wall
0	reference case

to the fuel reactor, where the fuel is oxidized in a N_2-free atmosphere. As in an oxyfuel combustion, the process produces reaction products undiluted with nitrogen, from which a concentrated CO_2 stream can be obtained by simple water condensation. At the same time, energy consumption for pure O_2 production via a cryogenic process is avoided. After the reaction with the fuel, the oxygen carrier is re-oxidized by reacting it with air, in a highly exothermic reaction which can be exploited for power generation. The single and overall reactions in CLC with syngas as fuel are listed in Eq. (1).

$$
\begin{aligned}
& n\,H_2 + n\,MeO && \rightarrow n\,H_2O + n\,Me \\
& m\,CO + m\,MeO && \rightarrow m\,CO_2 + m\,Me \\
& \frac{n+m}{2}O_2 + (n+m)\,Me && \rightarrow (n+m)\,MeO \qquad + \\
\hline
& n\,H_2 + m\,CO + \frac{n+m}{2}O_2 && \rightarrow n\,H_2O + m\,CO_2
\end{aligned}
\tag{1}
$$

The resulting overall reaction is equal to the fuel combustion reaction. So, the same amount of heat is released as during the conventional combustion, but in the case of CLC a separate CO_2-rich stream is obtained. Therefore, the CLC concept is an interesting possibility for power production combined with CO_2 capture.

Both solid, liquid and gaseous fuels are suitable for CLC (Adanez et al., 2012; Lyngfelt, 2013; Moldenhauer et al., 2014). In this work, coal is selected as primary feedstock, because it produces the largest amount of CO_2. Thus, applying CO_2 capture in power production from coal would result in the largest impact on mitigation of CO_2 emissions. Coal can be directly fed to the fuel reactor (Adanez et al., 2012; Lyngfelt, 2014; Mattisson et al., 2009) or first converted in a gasifier to syngas, which is afterwards fed to the CLC system. This study focuses on the second option. So, an integrated gasification chemical looping (IGCLC) process is considered, where the syngas production and treating are performed similarly to conventional integrated gasification combined cycle (IGCC) plants.

The heat produced with CLC has to be converted into electricity. The highest electrical efficiency when operating with clean gaseous fuels can be achieved by a combined cycle. Efficiency of combined cycles is very sensitive to the turbine inlet temperature. Therefore, the resulting gas stream from the oxidation stage has to be produced at high pressure (12–20 bar) and temperature (at least around 1200 °C) to achieve acceptable efficiencies. At these conditions, CLC in combined cycle configuration has conceptually proven to outperform the conventional CO_2 capture technologies, with the calculated efficiency of 3–5% points higher than with conventional CO_2 separation technologies (Erlach et al., 2011; Spallina et al., 2014).

In the CLC process, the particles react alternately with the fuel and with oxygen (from air). This alternated reactions can be achieved in several ways. The most studied method is by circulating the oxygen carrier particles between two interconnected fluidized bed reactors: a fuel reactor where fuel is oxidized and an air reactor where air is fed to oxidize the oxygen carrier. In this configuration

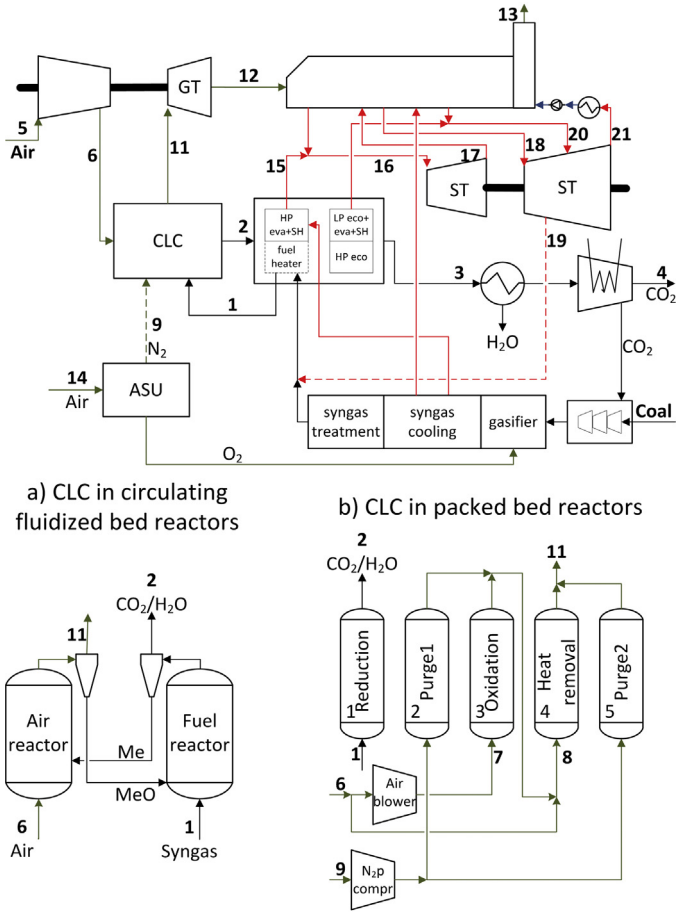

Fig. 1. Simplified scheme of the IG-CLC power plant and the circulating fluidized bed (a) and the packed bed configuration (b).

(illustrated schematically in Fig. 1a), the oxygen carrier is oxidized in the air reactor and here high temperature oxygen-depleted air is produced, which can be fed to the gas turbine. In the fuel reactor, the oxygen carrier is reduced with syngas and a stream of CO_2 and H_2O is continuously produced. Because of the continuous transport of oxygen carrier particles from one reactor to another reactor, the temperature difference between both reactors is small and depends on the solids circulation rate and on the enthalpy of fuel oxidation, which is often thermal neutral or slightly exothermic when syngas is used as fuel. The applicability of fluidized bed reactors at elevated pressure, needed to arrange a CLC based combined cycle, has been assessed in many process simulation studies (Wolf et al., 2005; Naqvi and Bolland, 2007; Consonni et al., 2006; Kjelstrup et al., 2007) but not demonstrated yet at significant scale. A critical aspect in this configuration is the need of maintaining a stable solids circulation between the two reactors and separating the fines inevitably entrained out of the cyclones with high temperature and high pressure filters before the gas is expanded in the turbine.

Alternatively, the oxygen carrier could be kept stationary while the gas flows are switched among different reactors, which can be achieved in a dynamically operated packed bed configuration (Fig. 1b) (Noorman et al., 2007, 2010). In this case, larger particles are used to avoid excessive pressure drops and to keep the particles stationary. Therefore, the risk of fines formation can be minimal and the separation between gases and solids is easier (or not required at all). The operation strategy in packed bed reactors is different from the one used in the interconnected fluidized beds and consists of the following five steps, schematically shown in Fig. 1b. (1) Starting with an oxidized oxygen carrier and a reactor temperature of 450–500 °C, the particles are reduced with syngas (reduction step). (2) The reactor is purged with N_2 to prevent contact between syngas and air (first purging step). (3) Air is fed to oxidize the particles again (oxidation step). During this process step, the bed temperature increases due to the exothermic oxidation reaction. (4) The heat is removed by blowing air through the bed and during this step, hot air is produced to feed the gas turbine (heat removal step). (5) At the end, of the cycle, the reactor is purged again to avoid air-syngas contact during the reduction step (second purging step). By operating multiple reactors in parallel, a continuous flow of fuel and air can be processed and a continuous production of the hot streams is achieved. To switch the gases at the outlet, a high temperature valve system should be available to distribute the gas streams to the right downstream sections, which is expected to be a costly part of the reactor control system. In the packed beds, the reduction can be carried out at lower temperature after the heat removal step, but it is also possible to change the operation order and carry it out at higher temperature before the heat removal step in case of low reactivity of the oxygen carrier (Spallina et al., 2014, 2013). In case the CO_2 and H_2O are produced at low temperature, more high temperature heat is available during the heat removal step, which can be used in the topping gas turbine cycle, which potentially increases the process efficiency. On the other hand, other issues like the impact of possible carbon deposition during reduction have to be considered as well.

Other CLC reactors configurations have been proposed in the literature, based on non-interconnected dynamically operated fluidized beds (Zaabout et al., 2013) and on a rotating bed reactor (Håkonsen and Blom, 2011; Håkonsen et al., 2014). These innovative concepts deserve to be considered in future works, but are not studied in this paper.

Although the two fluidized and packed bed concepts have been studied separately in some papers (Erlach et al., 2011; Spallina et al., 2014; Rezvani et al., 2009), the performances of both configurations have not been directly compared yet with the same assumptions and modeling tools. In this work, the packed bed and the fluidized bed reactor configurations are directly compared for the first time in terms of overall plant efficiency. NiO/Al_2O_3 has been selected as oxygen carrier for this comparison, because it is suitable for high temperature operation and has fast kinetics even at moderate temperatures and it is hence suitable for both reactor configurations (Adanez et al., 2012; Hamers et al., 2013).

The paper opens with a description of the IGCC power plant in which the CLC reactors are implemented. Subsequently, the packed bed configuration is discussed, including a sensitivity analysis regarding the steam addition (to avoid carbon formation) and the pressure drop (to reduce the number of reactors). A preliminary estimation of the initial investment costs is made to conclude which parameters (L/D reactor reaction, cycle time, oxygen carrier) are critical in the packed bed CLC reactor design. Finally, the process performance in the fluidized bed reactors is discussed. Because many papers have been published about circulating fluidized bed systems, the discussion is less extensive than the packed bed discussion. In the end, both configuration are compared.

2. IGCLC plant description

The IGCLC power plant including the CLC reactors has been evaluated with the GS (Gas Steam cycles) software developed at the Department of Energy of Politecnico di Milano (GECOS, 2013). This is a modular software, which allows modeling complex plant configurations for power generation and industrial processes. One of the main features of the code, useful for this application, is the calculation of gas and steam turbines with a

stage-by-stage approach, estimating the cooling flows required in each gas turbine blade row and accounting for the associated performance penalties (Chiesa and Macchi, 2004). The reactors are calculated based on thermodynamic equilibrium. NASA polynomials are used to describe the thermodynamics of the gases and solids and the water/steam properties are taken from Schmidt (1982).

A simplified overview of the IGCLC power plant is given in Fig. 1. This figure is mainly focused on the CLC and the power production sections of the process. For a more detailed overview and a complete description of the power plant, the reader is forwarded to Spallina et al. (2014). This paper contains all the assumptions the study is based on and a complete mass balance of the IG-CLC system (Spallina et al., 2014).

Bituminous South African Douglas coal has been selected as fuel for the Shell gasifier. Before it is fed to the gasifier, coal is dried from 8 to 2 wt%. The heat for this drying is provided by combustion of a small amount of dry cleaned syngas. The coal has to be pressurized and this is done in the lock hoppers with CO_2. Conventionally, N_2 is used to pressurize the solid fuels in Shell gasifiers of IGCC plants, but in that case the syngas would become too diluted, reducing the final CO_2 purity. About 35% of the CO_2 fed to the lock hoppers is introduced in the gasifier together with the fuel, the remaining is for 90% recovered and for 10% vented.

Coal is gasified in the Shell gasifier with oxygen and intermediate pressure steam as gasification agents. The gasifier is cooled by producing some intermediate pressure steam in membrane waterwalls. The oxygen (95% purity) is provided by a stand-alone air separation unit (ASU) based on a pumped liquid oxygen process consuming 325 kWh/t_{O_2} (IEA, 2005). In the gasification island also some N_2 is used and released with the vented CO_2 at the lock hoppers.

The syngas exiting the gasifier is cooled down to 900 °C by quenching it with a downstream colder recycled syngas. Afterwards, the syngas is cooled down while high pressure superheated steam is produced at 400 °C and sent to a scrubber. Sulfur is present as H_2S and COS. The COS is converted into H_2S in a catalytic packed bed that operates at 180 °C before the H_2S is removed with a Selexol solvent at ambient temperature. The H_2S is recovered via the Claus process where elemental sulfur is formed.

The pressure of the desulfurized syngas is first reduced to 21.6 bar and then the syngas is fed to the saturator to heat up the stream again and to increase the steam content. Subsequently, it is heated up to 300 °C with high pressure saturated water, before it is mixed with steam, added to avoid carbon deposition inside the reactors. Then the syngas is heated up to 600 °C in a heat exchanger with fuel reactor off-gases, before it is fed to the reduction reactor (#1). The produced CO_2-rich stream (#2) is cooled down in the heat recovery section. The heat released from the CO_2/H_2O stream is used to produce high pressure steam and superheat the steam produced in the syngas coolers from 400 °C to 565 °C (#15). The temperature gradients of the hot CO_2 released from the CLC unit (see discussion in Section 3) will probably require strategies to control the temperature variations of the tubes surface, which would otherwise suffer high thermal fatigue. This could be achieved for example by a proper arrangement of the heat transfer banks, by a controlled mixing with recycled cooler CO_2 or by buffering with inert material in a fixed or fluidized bed vessel, which could average the heat exchanger inlet temperature. Below 349 °C, water is economized, low pressure steam is generated and the water for the saturator is heated up to a maximum of 179 °C. Then, the steam is condensed and the CO_2 is intercooled compressed in 3 stages and finally pumped to 110 bar.

For the oxidation and heat removal in the CLC reactors, air is required. Before it is fed to the CLC reactors, it is compressed from the atmosphere to 20 bar (#6). The pressure drop is initially assumed equal to 5% of the inlet pressure. In the packed bed configuration, two additional streams are required. First, the air for the oxidation (#7) is slightly extra pressurized, because the outlet air is reused for the heat removal, as shown in Fig. 1. Second, N_2 is required to purge the reactors (#10) and this is obtained from the ASU (#9). As outlet stream from the CLC reactors, oxygen depleted air at 1200 °C is obtained (#11) and this is first expanded in the gas turbine and then it is fed to the heat recovery steam cycle (HRSC, #12), where steam is produced at three different pressure levels. At the end of the process, the depleted air is released to the ambient from the stack (#13).

Table 1
Properties of the NiO/Al_2O_3 used in the packed bed reactors for operations at 20 bar.

Oxygen carrier	19 wt% NiO/Al_2O_3 [a]
Particle size	10 mm
Solid bulk density	1031 $kg/m^3_{reactor}$
Void fraction	0.4 $m^3_{gas}/m^3_{reactor}$

[a] The required active weight content to reach 1200 °C depends on the operating pressure. For an operating pressure of 22–14 bar, the active weight content of NiO should be within a range of 18.5–20 wt%.

3. Packed bed configuration

The behavior in the packed bed reactors has been described by a 1D numerical model (Noorman et al., 2007). With this model, the temperatures of the gases exiting the packed bed reactors were determined. In this work, the Ni-based oxygen carrier in the packed bed reactors has the properties shown in Table 1.

During one complete process cycle, a profile as illustrated in Fig. 2 was obtained. When the reduction is started, the end of the bed still contains some heat from the previous cycle. This heat is blown out of the bed and therefore a decreasing outlet temperature profile is observed during the reduction step. The rest of the reactor has a temperature of 466 °C, which is the gas inlet temperature during the heat removal step for a pressure ratio of 20. For reduction of syngas with nickel, the selectivity toward CO_2 and H_2O is an issue at high temperatures (Jerndal et al., 2006), but at 466 °C complete fuel conversion is achieved. To achieve a steady high temperature gas stream to be fed to the gas turbine, several reactors are operated in the same step. Hence, the streams leaving the reactors are mixed and the temperature is equalized, obtaining temperature profiles like in Fig. 3. During the reduction step, the average CO_2/H_2O temperature is 832 °C. During the first

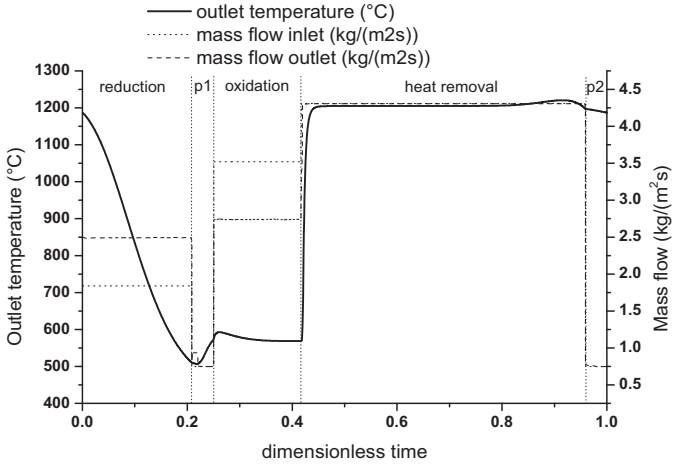

Fig. 2. Outlet temperature profile during packed bed CLC with NiO/Al_2O_3 as oxygen carrier (Hamers et al., 2014). p1 is purge 1 and p2 is purge 2.

Table 2
The considered costs of the reactors components for different cycle times and L/D.

Cycle time, min	10	20	40	60	90	20 ($L/D=2$)
L/D-ratio	4	4	4	4	4	2
Number of reactors	123	67	39	29	22	21
Reactor length, m	4.6	7.1	10.7	13.5	17	6.6
Reactor inner diameter, m	1.15	1.78	2.68	3.38	4.25	3.3
Thickness refractory, mm	306	383	495	579	692	182
Thickness steel, mm	16	23	33	40	50	33
Reactor costs, k€/reactor	12	37	110	208	397	60
High temperature valves, k€/valve	150	216	299	357	421	433
Oxygen carrier, €/ton				6000–50,000		

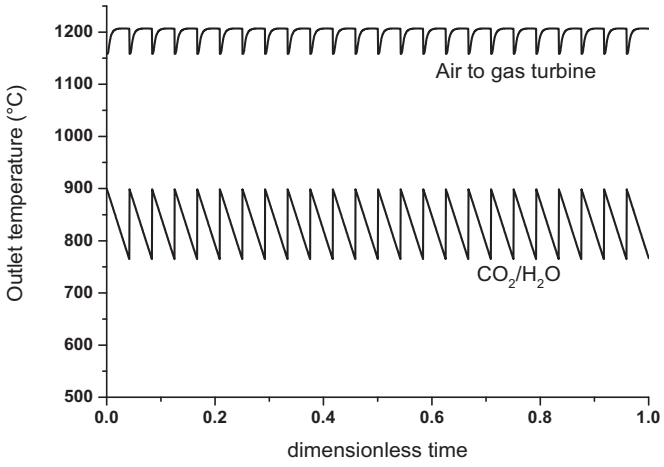

Fig. 3. Average outlet temperature of the air sent to the gas turbine and the produced CO_2/H_2O stream. In this situation, 4 reactors work in parallel for the oxidation, 5 for the reduction, 13 for the heat removal and 2 in purge mode are employed, as results from the dimensioning criteria presented in Section 3.3.

purge and the oxidation, the outlet temperature is between 500 and 600 °C. This gas stream is reused for the heat removal. During the heat removal a gas stream is produced with a temperature of 1200 °C.

Only the CO_2 that is produced during the reduction is captured. In case the carbon deposition reaction occurs, carbon is formed during reduction and combusted during oxidation, leading to a lower carbon capture efficiency. It might also be that the oxygen carrier degrades due to the formation of carbon deposits. Hence, the extent of the carbon deposition reaction should be reduced as much as possible. In this base case configuration, a certain amount of steam is fed so that, according to the thermodynamic equilibrium calculations, no carbon deposition can occur at a temperature above 450 °C. This is achieved by mixing 33.4 kg/s steam with the syngas after the saturator. This has quite some impact on the process efficiency, as it will be described below. In the following sections, a sensitivity analysis is carried out on this particular and crucial point.

Based on the obtained outlet temperatures and the amount of steam mixed with the syngas, the IGCLC power plant mass and energy balances have been calculated. The stream table of the IGCLC plant with packed bed CLC is shown in Table 3 and the corresponding simplified plant scheme is displayed in Fig. 1. The overall efficiency is 41.05% on LHV basis and CO_2 capture is around 97%. More detailed information about the energy balance is given further in Section 4.

In the following sections, the results of a sensitivity analysis are reported, carried out on the method used to avoid carbon deposition, the pressure drop and the gas turbine pressure ratio.

3.1. Carbon deposition prevention method

Carbon deposition could occur by the Boudouard reaction,[1] Eq. (2).

The equilibrium of this reaction favors carbon formation at high pressure and low temperatures. Since the reduction is carried out at relatively low temperature in the packed beds and the fuel is in contact with a reduced oxygen carrier (i.e. no additional oxygen can be released to the gas phase by the oxygen carrier), carbon deposition could occur in the reactor. Carbon deposition can be prevented by recycling CO_2 and H_2O and/or by adding steam which favor the C consumption through the gasification reaction, Eq. (3). In the case a H_2O/CO_2 stream is recycled, the outlet stream of the packed bed reactors is cooled down to 450 °C and then some H_2O/CO_2 is slightly pressurized by a blower and sent back to the reactor inlet. Increasing the flow rate of the recycle stream means that a larger flow enters the CLC reactors, which absorbs a higher amount of heat and has to be cooled down. Hence, more high pressure steam is produced and a lower amount of heat can be extracted during the heat removal phase.

$$2CO \rightleftarrows CO_2 + C \qquad \Delta H_R = -172.4\,\text{kJ/mol} \tag{2}$$

$$C + H_2O \rightleftarrows CO + H_2 \qquad \Delta H_R = +131.3\,\text{kJ/mol} \tag{3}$$

The effects of the different recycle ratios on the steam to be added to avoid carbon deposition are reported in Fig. 4. To draw this figure, a minimum temperature of 450 °C in the Boudouard equilibrium calculations is assumed to prevent carbon deposition in the bed. Such a syngas dilution is also expected to be sufficient to prevent metal dusting in CLC fuel heater, where syngas is heated up to 600 °C (a temperature range where metal dusting corrosion can occur) (Natesan and Zeng, 2003). Here it is shown that if the recycle ratio is increased, less additional steam is required to avoid carbon deposition. Moreover, if only a recycle is used, with no dilution with steam from the steam turbine, a very large stream has to be recycled (about 2.75 times the CO_2/H_2O mass flow rate), because CO_2 is not as effective to prevent carbon deposition as steam. Increasing the recycle leads to an increase of the high pressure steam produced from CO_2/H_2O cooling. To provide sufficient saturated water, the ΔT at the pinch point has to be increased with detrimental effects on process efficiency. Therefore, cases requiring increased ΔT are not reported in Fig. 4 and curves are interrupted at a certain value of the recycle ratio.

Fig. 4 also demonstrates that in case a larger recycle ratio is selected, the flow to the gas turbine is decreased, with negative effects on the process efficiency: increasing the exhaust recirculation, results in a higher HP steam production in the first heat exchangers after the reactor operated in reduction, which decreases the overall thermal input of the CLC unit and thus, limits the heat

[1] The reaction enthalpy has been calculated at standard conditions with the thermodynamics data taken from Barin (1993).

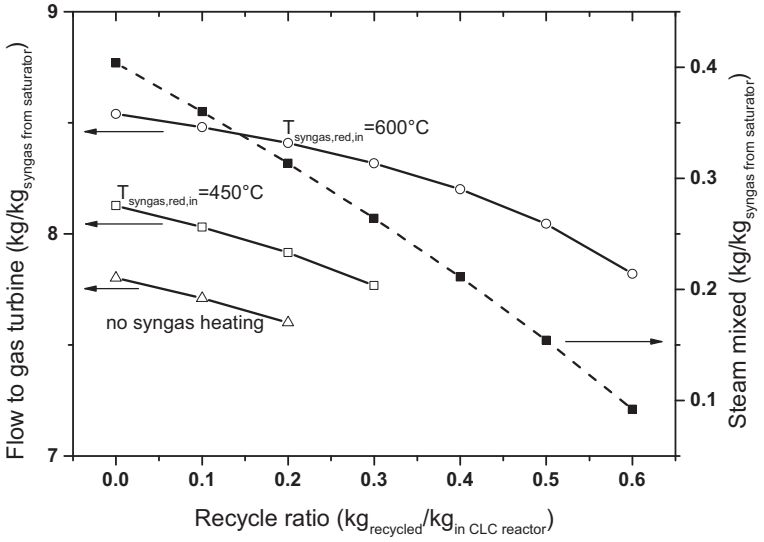

Fig. 4. The gas turbine inlet flow rate and the amount of steam mixed at different recycle ratios.

available for the topping gas turbine cycle. The same effect occurs with lower preheating temperatures of the syngas to the CLC unit since a higher portion of the heat of reaction is needed for heating the syngas up to the reaction temperature (as shown in the figure). Another effect of the CO_2/H_2O recycle is related to the electricity consumed by the recycle blower to compensate the pressure drop inside the reactors and the CO_2 cooler. These effects are partly balanced by the higher production rate of high pressure steam, which increases the electricity produced by the steam turbine. On the other hand, a reduction of the amount of steam needed for syngas dilution has a positive effect on the steam cycle efficiency, since a higher amount of steam is expanded in the turbine down to the condensing pressure, instead of being mixed with the syngas and eventually condensed at higher temperature during the CO_2-rich stream cooling.

The result of these effects is illustrated in Fig. 5, where the process efficiency is shown as a function of the recycle ratio. It turns out that the size of the recycle flow has a relatively small effect on the process efficiency. The case without recycle has been selected as base case, because this is the case with the minimum flow sent

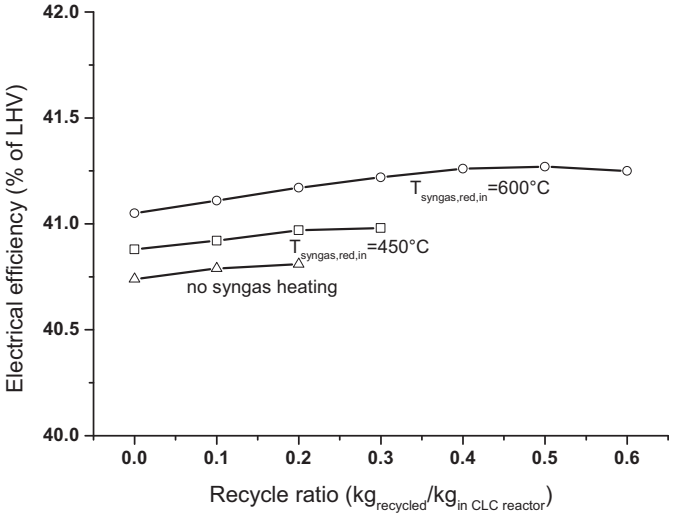

Fig. 5. The influence of the recycle ratio and the syngas feeding temperature on the process efficiency.

to the reduction reactor and its efficiency is only about 0.25% points lower than the optimal case when a syngas preheating temperature of 600 °C is adopted.

Syngas preheating before feeding the CLC reactor system is performed by cooling the CO_2/H_2O stream. In addition to the improved process performance, increasing the syngas inlet temperature to 600 °C has another advantage. The inlet temperature is closer to the temperature in the reactor after the reduction reactor. Therefore, only a small temperature change is observed and this leads to fewer temperature fluctuations in the gas turbine inlet stream. A drawback of this heating procedure is that it is achieved in a gas/gas heat exchange, which is expected to require a relatively large surface area.

In the above mentioned cases, a conservative estimation was selected for the amount of steam needed to avoid carbon deposition, because the thermodynamic equilibrium was followed. However, the kinetics determine how fast a reaction occurs and based on this, it might be that a smaller amount of steam is sufficient to avoid carbon deposition (or limit it to acceptable levels). The effect of a small amount of carbon deposition on the process thermodynamics is small. If 1% of the CO is deposited (evenly distributed) in the bed, the temperature rise during oxidation increases by 2 °C.

If no additional steam and no recycle are fed with the mixture, still a H_2O/CO-ratio of 0.37 is fed to the reactor (#1) thanks to the humidification obtained in the saturator. So, the carbon formation reaction is suppressed to a certain extent and this might be sufficient in case the kinetics of carbon deposition are slow. This leads to an efficiency that is 1.18% point higher (42.23% of LHV). So, the effect of adding steam or using a recycle is quite significant. Therefore, the kinetics of the Boudouard reaction are an important aspect in the selection of the oxygen carrier for the packed bed process and should be investigated experimentally. In Fig. 6 the effect of the added steam on the process efficiency is displayed.

For final considerations, the results just presented can be compared with the outcomes of a similar analysis performed in Spallina et al. (2014). In that case, a much more pronounced dependence of plant efficiency on both the CO_2/H_2O recycle and steam dilution, in order to avoid carbon deposition, was obtained. The first reason of the lower dependence obtained in this work is related to the lower average temperature of the CO_2/H_2O stream produced in the plant assessed in this work, which limits the effect of higher fuel flows on the hot air flow rate to the gas turbine. As a matter

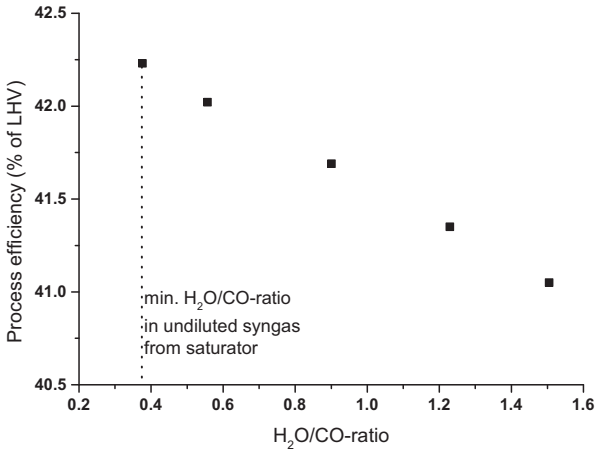

Fig. 6. The process efficiency as a function of the amount of steam mixed with the syngas. Initial H_2O/CO ratio of undiluted syngas from the saturator is equal to 0.37. At a H_2O/CO-ratio of 1.5, carbon deposition cannot occur according to thermodynamic equilibrium at 450 °C and higher.

of fact, in Spallina et al. (2014) a different packed bed operation sequence is adopted to manage the lower kinetics of ilmenite on CO oxidation and the reduction step is performed on the hot bed just after the oxidation phase. Therefore, the CO_2/H_2O stream is also produced at a significantly higher temperature. The second reason is related to the configuration of the heat recovery section for the CO_2/H_2O stream, which consists in this case of a low pressure evaporation level, which can recover the increasing low temperature heat originating from steam condensation when high steam dilution is adopted. In Spallina et al. (2014), such a LP evaporation level is not present and low temperature heat from steam condensation is not recovered as efficiently.

3.2. Compression ratio and pressure drop in packed bed reactor

The effect of the compression ratio and the pressure drop is illustrated in Fig. 7. It is demonstrated that the compression ratio has little effect on the process efficiency. A compression ratio of 20 was selected, corresponding to the highest plant efficiency. In addition to efficiency, the pressure ratio influences the design and operation of the reactor system in two ways. First, a higher bed temperature during reduction is obtained in case of a higher compression ratio. In an adiabatic compression, the higher the final pressure, the higher the final temperature. Since a compressed air stream

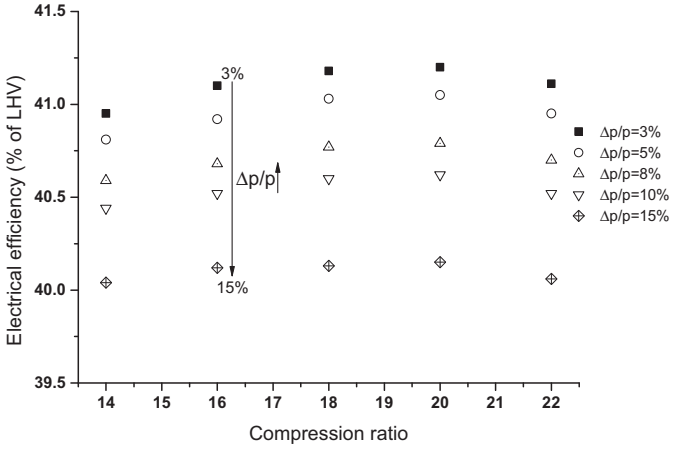

Fig. 7. The effect of the compression ratio and the pressure drop on the process efficiency.

is fed to the CLC reactors for the oxidation and the heat removal, when the reduction starts, the bed temperature is equal to the heat removal gas inlet temperature. For the reduction reaction rates, the temperature is quite a critical parameter and therefore a higher compression ratio is beneficial. Second, a higher pressure ratio leads to a higher gas density and therefore a larger gas mass flow rate can be sent through the reactor for a given pressure drop. As it will be demonstrated in the next section 3.4, the number of reactors needed is lowered by increasing the compression ratio.

For the plant assessed, the optimal compression ratio of 20 is higher than expected for the turbine inlet temperature (TIT) of 1200 °C, based on the experience on conventional natural gas-fired combined cycles. As a matter of facts, optimal pressure ratios are around 12–14 in combined cycles utilizing a gas turbine with a turbine inlet temperature in that range. The higher than expected optimal pressure ratio is due to two reasons: (1) the maximum SH steam temperature is only slightly influenced by the pressure ratio, since most of the steam is superheated by hot CO_2 from the CLC reactors; (2) CO_2 compression consumption reduces when operating the reactors at a higher pressure.

In Fig. 7 the effect of the pressure drop is shown as well. A larger tolerated pressure drop inside the reactors results in a lower process efficiency, because the stream fed to the gas turbine has a lower pressure in that case. In case the gas turbine inlet pressure is lower, the outlet temperature is higher. Therefore, steam produced in the heat recovery steam cycle (HRSC) can be superheated and reheated to a higher temperature since a fixed temperature approach of 25 °C is considered between the gas entering the HRSC and the final superheater and reheater temperatures.

What pressure drop should be tolerated depends on the process economics, since higher pressure drops lead to higher allowable gas velocities and hence a lower number of reactors. This analysis is out of scope of this work but deserves certainly more attention in a future research.

3.3. Reactor design strategy

The packed bed process can be made continuous by running several beds in parallel. In this section, the scaling of the reactor and the required number of the reactors is determined. For a continuous process, no buffers should be required. So, a continuous inflow of reactants and outflow of hot air and CO_2 should be facilitated. Hence, at least one reactor should be in each operation step, which means that for this process, at least five reactors are required. For some operation steps, a larger number of reactors is needed, because otherwise the flow rate and the velocity in each reactor are too high to keep the pressure drop within the given constraints.

The following strategy is used to determine the size of the reactors and the number of reactors. First, a certain cycle time is set, notably 20 min. This number is varied in Section 3.5. Very short cycle times should be avoided to reduce the losses during purging steps and avoid too quick valve switching. For this time, sufficient oxygen carrier should be available to facilitate the indirect combustion of syngas. The total reactor volume can be calculated by multiplying the molar flow rate of the fuel ($\dot{m}_{H_2} + \dot{m}_{CO}$) by the total cycle time (total time of all the operation steps) and dividing it by the amount of atomic oxygen per m^3 reactor, as illustrated in Eq. (4). The total reactor volume (volume of each reactor multiplied by number of reactors) should be close to this number.

$$V_R = \frac{(\dot{M}_{CO} + \dot{M}_{H_2}) \cdot \tau}{\rho_{mol,oxygen}} \quad (4)$$

The second parameter that determines the reactor dimensions is the pressure drop, which is calculated with the Ergun equation

(Ergun, 1952). A certain maximum tolerable pressure drop and reactor length are assumed and based on these the maximum specific flow rates (flow rate per cross-section square meter) in each step are set. The minimum number of reactors required for a certain operation step can be calculated by dividing the total capacity (in kg/s) by the maximum specific flow rate (kg/(m^{2}s)) and the reactor cross section (m^2). In this work, the reactor diameter is related to the length by fixing the *L*/*D*-ratio.

If the *L*/*D*-ratio is reduced for a fixed pressure drop, the overall reactors cross-section does not change because the specific flow rate remains constant. The effect of the decrease of the *L*/*D* is that the volume of each reactor increases and therefore the number of reactors can be reduced. In case a higher pressure drop can be tolerated, smaller cross-sections (i.e. higher specific flow rates) and longer reactors can be selected and therefore the number of reactors reduces.

Decreasing the number of reactors is expected to reduce the fixed costs also because of the reduced number of valves required. The following measures can be taken to decrease the number of reactors:

- Decrease the *L*/*D* ratio of the reactors. If the reactor diameter is increased, the footprint per reactor increases and then less reactors are needed to facilitate the desired flow. On the other hand, a uniform gas flow distribution along the reactor cross section can become difficult at low *L*/*D*. In addition, the reactor diameter should not exceed ca. 6 m, because transport might become problematic and the walls might become too thick.
- Increase the maximum permitted pressure drop. Increasing the maximum permitted pressure drop means that a larger specific flow rate can be used and the reactor length can be increased. Therefore, a smaller overall footprint is required and thus a lower number of reactors.
- Increase the particle diameter. For a given reactor diameter, the larger the particle diameter, the lower the pressure drop, the longer the reactors and the lower the number of reactors. For this parameter, an optimum has to be found between diffusion limitations inside the particles and costs.
- Increase the cycle time. This can be demonstrated on the basis of simple mathematical considerations, as follows. The total reactor volume is dependent on the amount of syngas that has to be processed during the time of a cycle, as shown in Eq. (4). The total reactor volume is by definition also equal to the number of reactors multiplied by the volume of one reactor (Eq. (5)). Based on a fixed *L*/*D*-ratio, Eq. (5) can be rearranged so that a function for the length can be formulated, which is given in Eq. (6). Eq. (7) demonstrates that the superficial gas velocity is equal to the mass flow rate (kg/s) divided by the gas density, the reactor cross section and the number of reactors in a certain step ($\varphi_{step}N_R$, where φ_{step} represents the portion of reactors operating in the considered step). When these terms are implemented in the Ergun equation, it is shown how the cycle time and the number of reactors correlate with the pressure drop (Eq. (8)). Considering only the design of the reactors, many parameters are constant (c_1, c_2, c_1' and c_2') and then it appears that in case the cycle time decreases, the number of reactors has to be increased.

$$V_R = N_R \cdot \frac{\pi}{4} \cdot D^2 \cdot L = \frac{(\dot{M}_{CO} + \dot{M}_{H_2}) \cdot \tau}{\rho_{mol,oxygen}} \tag{5}$$

$$L = \sqrt[3]{\frac{(\dot{M}_{CO} + \dot{M}_{H_2})}{\rho_{mol,oxygen} \cdot (\pi/4) \cdot (D/L)^2} \frac{\tau}{N_R}} \tag{6}$$

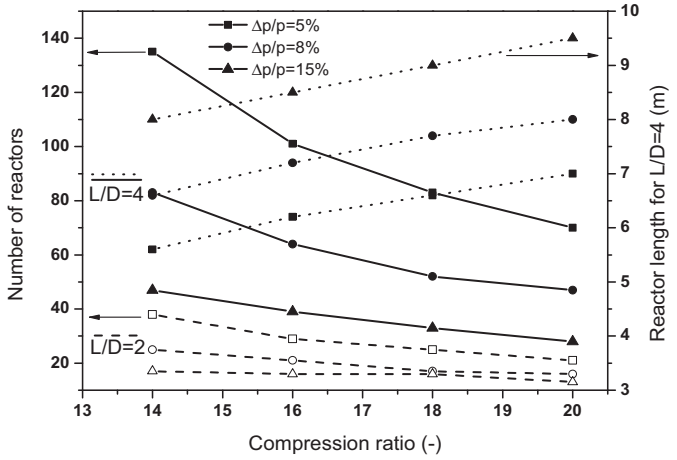

Fig. 8. The number of reactors as a function of the compression ratio with different *L*/*D*-ratios and pressure drops (cycle time is 20 min and 10 mm particle diameter). Because the cycle time is constant, the total reactor volume is also constant at 1183 m^3. For clarity, the reactor length is only shown for *L*/*D*-ratio of 4.

$$v_g = \frac{\dot{m}}{\rho_g \phi_{step} N_R (\pi D^2/4)} = \frac{\dot{m}}{\rho_g \phi_{step} ((\dot{M}_{CO} + \dot{M}_{H_2})/\rho_{mol,oxygen})(\tau/L)}$$
$$= \frac{\dot{m}}{\rho_g \phi_{step} ((\dot{M}_{CO} + \dot{M}_{H_2})/\rho_{mol,oxygen})} \frac{L}{\tau} \tag{7}$$

$$\Delta p = 150 \frac{\eta_g}{d_p^2} \frac{(1-\varepsilon_g)^2}{\varepsilon_g^3} v_g \cdot L + 1.75 \frac{\rho_g}{d_p} \frac{(1-\varepsilon_g)}{\varepsilon_g^3} v_g^2 \cdot$$
$$L = c_1 \frac{L^2}{\tau} + c_2 \frac{L^3}{\tau^2} = \frac{c_1'}{\tau^{1/3} N_R^{2/3}} + \frac{c_2'}{\tau \cdot N_R} \tag{8}$$

The influence of the pressure drop and the cycle time is further discussed in the next sections.

3.4. Effect of compression ratio on number of reactors

Based on the above mentioned strategy, the number of reactors has been calculated for each step of the CLC process and for different compression ratios. In Fig. 8 it is reported that less reactors are needed, if the compression ratio is increased for a specific pressure drop and *L*/*D*-ratio. In some cases, quite a large number of reactors is required and therefore it is important to select the operating conditions carefully. In all the considered cases, the total cycle time is 20 min. So, the amount of oxygen carrier, and thus the reactor volume, is always the same. Hence, when the reactor number is lower, the reactors are larger.When the *L*/*D*-ratio is reduced from 4 to 2, the diameter per reactor is larger and therefore fewer reactors are needed. In general, lower *L*/*D* ratios seem preferable to limit the total number of reactors and the ancillary components (e.g. piping, valves). On the other hand, the optimum *L*/*D*-ratio depends on the reactor production method, on how well the flow is distributed over the cross-section when *L*/*D* decreases and on the effects on temperature equalization of the outlet gas as discussed at the beginning of Section 3.

In general, 50–65% of the reactors are in the heat removal step, 2 reactors are in purge and about 20% are in reduction and about 20% are oxidation.

3.5. Influence of cycle time

In the previous calculation, a total cycle time was adopted of 20 min. The same procedure has been carried out for different cycle times and an overview of the results is given in Fig. 9. As explained

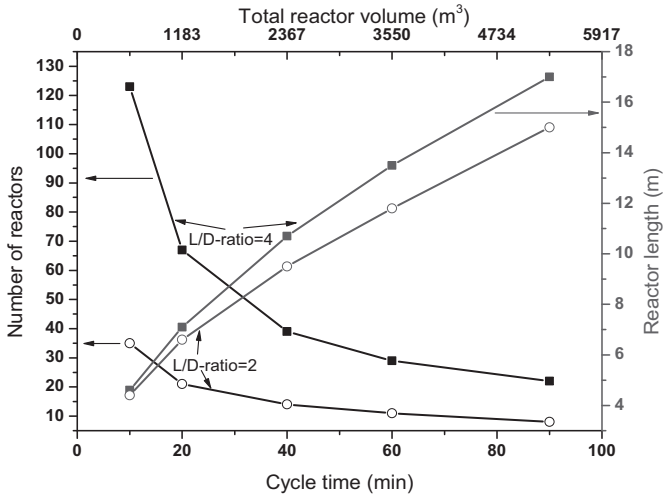

Fig. 9. The influence of the cycle time on the required reactor number and the reactor length (with *L*/*D*-ratios of 2 and 4).

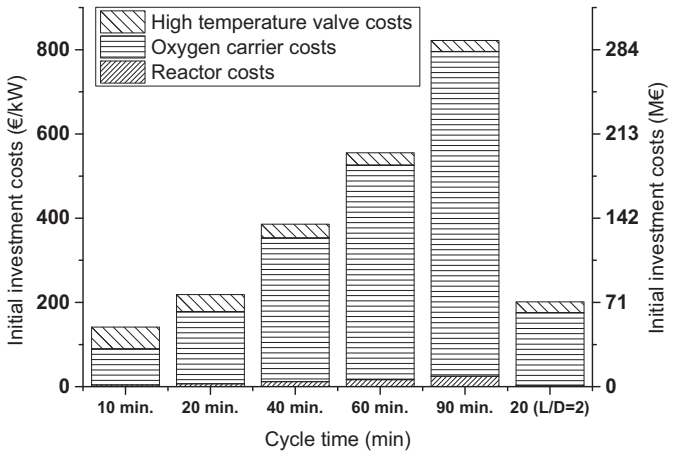

Fig. 10. Influence of the cycle time on the costs in case of NiO/Al_2O_3 (estimated on 50,000 €/ton NiO/Al_2O_3).

in Section 3.3, the longer the selected cycle time, the lower the number of reactors, the lower the number of high temperature valves required and the larger the reactors. Also in this case a fixed *L*/*D*-ratio of 4 was selected. Some examples of the reactor sizes are given in Fig. 9.

The solids inventory is dependent on the cycle time. If the cycle time is increased, more oxygen has to be available to process syngas for a longer time. Hence, the longer the cycle time, the higher the solid inventory.

In case of a short cycle time, the high temperature valves have to be switched more often. Therefore, the lifetime of the valves is expected to be lower. In the previous sections, a cycle time of 20 min was assumed. This corresponds to a total solids inventory of 1200 ton (1750 kg solid/MW_{th} = 261 kg Ni/MW_{th}), which means that 180 ton nickel is required.

3.6. Preliminary investment costs estimation

The impact of the cycle time, the *L*/*D*-ratio and the oxygen carrier on the initial investment costs has been evaluated by a simple preliminary economic analysis. It only includes the packed bed reactors with the oxygen carrier and the high temperature valves.

The cost of the high temperature three-way valve is estimated on 150,000 € per valve in case of the smallest reactors. The high temperature piping is included in the calculation. The valves have been scaled up by Eq. (9) (Seider et al., 2004), in which C_0 represents the reference costs of 150,000 €/valve in the 123 reactors case (with a flow rate of 2 m^3/s). In case of a smaller number of reactors, the volumetric flow rate per valve increases and then the valve size increases and therefore its costs. The costs of the high temperature valve system are listed in Table 2 for each cycle time.

$$C = C_0 \left(\frac{\dot{V}}{\dot{V}_0} \right)^{0.6} \tag{9}$$

The reactors contain an internal refractory, a steel vessel and an external refractory. The internal refractory is needed to protect the steel vessel, for which a maximum temperature of 300 °C has been assumed. The thickness of the refractory, s_r, is calculated using Eq. (10), which results from the energy balance on the insulation material around the reactor wall and the law of Fourier. It is assumed that the total heat losses through the reactor walls of all the reactors, *Q*, are equal to 1.5 MW (with thermal conductivity of refractory, λ_r, of 0.2 W/(m K)). This is about 0.25% of the total heat production and therefore this term is not included in the energy evaluation of the power plant. The carbon steel thickness of the pressurized vessels has been calculated with Eq. (11) (Sinnott, 2005), in which P_{in} is the operating pressure (30 bar assumed for safety reasons), D_a is the diameter of the reactor and the refractory and *f* is the design stress (85 N/mm^2 (Sinnott, 2005)). At the inlet and outlet of the reactors, hemispheres have been considered. The cost of the external low temperature refractory (around the pressurized vessel) has been neglected. The costs of the vessels are calculated considering steel costs of 500 €/ton (WSP, 2014) and fire bricks (refractory) of 450 €/ton (density of 480 kg/m^3, (ThermalCeramics, 2013)). The total material costs are multiplied with a factor 3 for the construction of the reactors. The resulting internal refractory and steel vessel thicknesses and their associated costs have been listed in Table 2.

$$Q = \frac{2\pi\lambda L}{\ln\,(D_a/D)}(T_{max,CLC} - T_{steel}) \tag{10}$$

$$s_{steel} \geq \frac{P_{in} D_a}{4f - 1.2P_{in}} \tag{11}$$

The nickel based oxygen carrier price was estimated at roughly 50,000 €/ton carrier. The different cost assumptions are listed in Table 2. From Fig. 10 it can be concluded that the Ni-carrier is, by far, the most expensive part of the system. This leads to design guideline to reduce the cycle time as much as possible.

Nickel is considered as one of the most expensive oxygen carriers and cheaper alternatives might be selected. For example if a natural material is selected (cost estimated at 6000 €/ton, mainly costs of palletizing), the contribution of the high temperature valves on the total cost becomes important. Reducing the cycle time means increasing the number of reactors and then the high temperature valves are the most expensive parts of the system. In Fig. 11 it is shown that if the cycle time is increased, the oxygen carrier costs become more dominant, because they increase linearly with the cycle time, while the number of reactors decreases (and thus the number of high temperature valves). So, in case of an expensive oxygen carrier (like nickel), the solid inventory has to be reduced as much as possible and in case of a cheaper material it is also important to keep the number of reactors low.

The case with a 20 min cycle time is also shown in case of a *L*/*D*-ratio of 2 (instead of 4) in Fig. 11. In that case, the system can be operated with a smaller number of reactors (and high temperature valves) and then the initial investment costs can be further reduced.

The specific investment costs for an IGCC power plant are around 1950 €/kW_{net} and for a plant with CO_2 capture, these costs rise to around 2650 €/kW_{net} (Anantharaman et al., 2011). The initial investment costs of the packed bed reactor systems for the CLC are lower than the 700 €/kW_{net}. So, the order of magnitude

Table 3
Comparison streams in packed bed and fluidized bed configuration (stream numbers, #, refer to Fig.1).

Stream #	Packed bed configuration				Fluidized bed configuration			
	M, kg/s	*T*, °C	*p*, bar	Composition	*M*, kg/s	*T*, °C	*p*, bar	Composition
1	116.3	600	20.1	Ar: 0.55%, CO: 32.09%, CO_2: 5.28%, H_2: 13.07%, H_2O: 48.29%, N_2: 0.72%	72.7	300	20.1	Ar: 0.97%, CO: 56.41%, CO_2: 9.27%, H_2: 22.97%, H_2O: 9.11%, N_2: 1.27%
2	156.9	832	19.0	Ar: 0.55%, CO_2: 37.37%, H_2O: 61.36%, N_2: 0.72%	113.3	1295	19.0	Ar: 1.01%, CO_2: 65.64%, H_2O: 32.07%, N_2: 1.29%
3	156.9	136	18.0	Same as #2	113.3	138	18.0	Same as #2
4	81.5	28	110.0	96.70% CO_2	81.5	28	110.0	96.63% CO_2
5	786.2	15	1.0	Air: Ar: 0.92%, CO_2: 0.03%, H_2O: 1.03%, N_2: 77.28%, O_2: 20.73%	695.3	15	1.0	Air
6	729.8	438	20.0	Air	645.1	438	20.0	Air
7	176.6	448	21.0	Air	–	–	–	–
8	698.4	466	20.0	Depleted air: Ar 0.94%, CO_2: 0.03%, H_2O: 1.06%, N_2: 81.86%, O_2: 16.11%	–	–	–	–
9	18.4	22	1.1	N_2	–	–	–	–
10	18.4	478	20.4	N_2	–	–	–	–
11	707.6	1199	19.0	Same as #8	605.5	1200	19.0	Depleted air: Ar 0.97%, CO_2: 0.03%, H_2O 1.10%, N_2: 81.81%, O_2: 16.09%
12	764.0	486	1.0	Depleted air: Ar 0.94%, CO_2: 0.03%, H_2O: 1.06%, N_2: 81.52%, O_2: 16.45%	655.8	487	1.0	Depleted air: Ar 0.97%, CO_2: 0.03%, H_2O 1.09%, N_2: 81.46%, O_2: 16.45%
13	764.0	92	1.0	Same as #12	655.8	86	1.0	Same as #12
14	120.7	15	1.0	Air	125.2	15	1.0	Air
15	88.6	565	133.9	Steam	133.1	565	133.9	Steam
16	129.5	527	133.9	Steam	156.0	547	133.9	Steam
17	129.5	333	36.0	Steam	156.0	349	36.0	Steam
18	142.6	458	33.1	Steam	160.4	458	33.1	Steam
19	33.4	395	21.6	Steam	–	–	–	–
20	37.7	300	3.5	Steam	0.3	300	3.5	Steam
21	146.8	32	0.05	Steam	160.7	32	0.05	Steam

of the reactor system costs is acceptable compared to the total plant cost. However, to draw more accurate conclusions a detailed economic evaluation has to be carried out on the complete plant, which also includes the operational costs and a sensitivity analysis on the most critical components. An important component is the high temperature valve system, which cost also depends on the operational cycle time. From this simple preliminary analysis, it can be concluded that the solid inventory is very important for the costs in case nickel is used as oxygen carrier. The oxygen carrier also needs to be replaced after a while and this will have an effect on the operational costs. If a cheaper oxygen carrier is selected, the number of reactors also becomes an important design factor to keep the number of high temperature valve systems as low as possible.

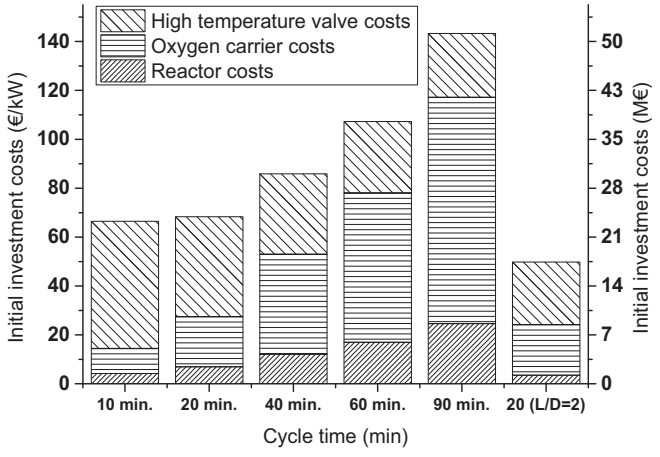

Fig. 11. Influence of the cycle time on the costs in case of a cheap oxygen carrier (6000 €/ton oxygen carrier).

Because no cost information was available about cyclones, the investment cost has only been estimated for the packed bed configuration.

4. Fluidized bed configuration

4.1. Reactors operation and solid inventory

Because many papers have been published about circulating fluidized bed systems, the discussion is less extensive than the packed bed case. An ideal fluidized bed system is considered, assuming that it is working at 20 bar without producing fines. If it would be operated at atmospheric pressure, it would not be a fair comparison.

In the configuration with circulating fluidized beds the temperature rise inside the reactor is independent of the active weight content, since it can be controlled by gas excess (or by immersed heat transfer surfaces in case of steam generation). As a matter of fact, thanks to the good mixing of the bed material, small temperature gradients prevail in the reactors without risk of hot spots formation. Therefore, a higher active weight content could be selected than 19 wt% NiO on Al_2O_3, optimized on chemical and mechanical stability rather than imposed by temperature rise control. In the literature, an active weight content of 40 wt% is commonly selected (Adanez et al., 2012).

The conversion of the oxygen carrier is something that distinguishes fluidized beds and packed beds. In the packed bed configuration the carrier is almost fully converted ($\Delta X_s = 1$), while in the fluidized bed the oxygen carried by the metal oxide is utilized only for a certain extent. On the one hand, due to the large air excess in the air reactor, the metal is expected to leave the air reactor in fully oxidized state. Conversely, since the highest possible oxidation of the fuel needs to be achieved in the fuel reactor, the oxygen carrier cannot be completely reduced in fluidized bed fuel

reactor and a certain amount of it needs to be kept in the oxidized state. The composition of the solids inside the fuel reactor determines the reactivity of the bed and the solids inventory required to reach full conversion of the syngas. Based on the selected oxygen carrier conversion and on the gas flow rates, the needed solids circulation rate can be calculated. Typically, the solid conversion ΔX_s is maintained below 0.5 to keep a good reactivity of the fuel reactor bed. At elevated pressures, the gas transport capacity of the solids is limited by hydrodynamics, because the reactors have a smaller cross sectional area (Abad et al., 2007). Owing to the low transport of solids, a relatively large ΔX_s should be selected, or alternative solid transport systems between the reactors should be employed to keep a sufficiently high solids circulation rate.

Abad et al. (2007) and Mattisson et al. (2007) calculated the solids inventories at around 70 kg/MW_{th}. This value is calculated based on a ΔX_s of 0.5 and the kinetics at 1200 °C and 20 bar. The calculation only includes the air and the fuel reactors and thus the solids inventory of the total system (including cyclones and loop seals) is higher. The solids inventory in the fuel and air reactor corresponds to 375 mol_{NiO}/MW_{th}. Considering that 1 MW_{th} thermal input corresponds to 3.7 mol_{CO-H_2}/s (with $CO/H_2 = 2.46$ as in our IGCC), it means that the total residence time of the oxygen carrier in the two reactors is 51 s (assuming $\Delta X_s = 0.5$).

Another solids inventory was found based on experiments carried out by Kolbitsch et al. (2010). During small scale experiments (65 kW) a solids inventory of 450 kg/MW_{th} (141 kg Ni/MW_{th}) was sufficient to convert H_2 with nickel oxide (40 wt% NiO on $NiAl_2O_4$) (Kolbitsch et al., 2010, 2009). A total residence time in the system of 130–350 s was reached. The ΔX_s was about 0.1 (Kolbitsch et al., 2010), so quite low in comparison with the above described situation.

In both cases, a lower active weight content was reported than was assumed for the packed bed case. The required solids inventory is lower in the case of circulating fluidized beds, because the residence time of the solids is lower (a couple of minutes) than the time of a packed bed cycle. The oxygen carriers in the packed bed reactors are most of the time not in a reacting mode (reduction and oxidation), but in the heat removal and purge mode. These steps, not needed for the fluidized bed reactors, make the total cycle time longer.

The difference in solids inventory might be compensated to a certain extent by a longer lifetime. The carriers in the packed bed are exposed to much less mechanical stresses and therefore the lifetime might be longer. At this moment, the difference in lifetime in both reactors is unclear and needs to be further explored experimentally.

4.2. IGCLC configuration with circulating fluidized beds

For the interconnected fluidized bed case, the IGCLC power plant configuration is slightly different from the case with packed bed reactors on four aspects:

First, the temperature of the fuel reactor is close to the air reactor temperature, because of the circulation of the solids that transfer a large amount of heat between the two reactors. Because of the high fuel reactor temperature and the highly uniform temperature in the reactor, the equilibrium of the Boudouard reaction is more on the CO side (no carbon formation). In addition, the oxygen carrier is not fully reduced and well mixed and some oxidized carrier is hence expected to be available in each zone of the fuel reactor. Therefore, carbon deposition is not considered to be a critical issue in fluidized beds and fuel dilution with steam or recycled CO_2 is not needed in this case.

Second, the oxidation and the heat removal steps are integrated in one step. During oxidation, a large excess of air is fed at 440 °C, only a fraction of the oxygen is reacting (about 25%) and a stream is obtained at 1200 °C. This temperature is reached by tuning the air gas flow rate. Only one compressor is required to obtain the air at 20 bar. So, no additional blower has to be installed for the oxidation.

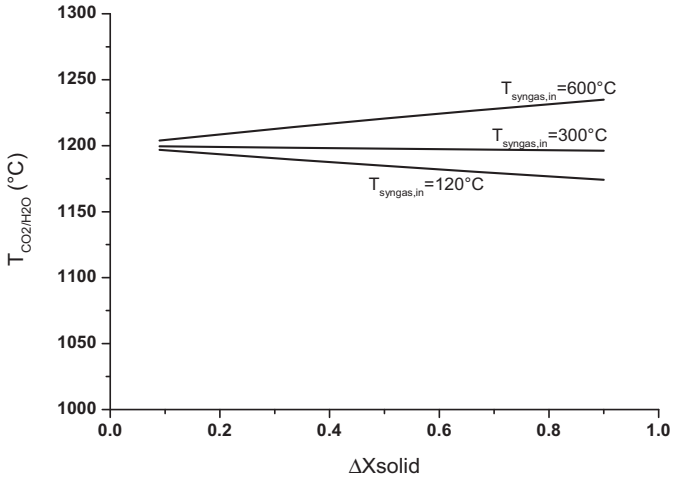

Fig. 12. The fuel reactor temperature as function of the solids conversion and the fuel inlet temperature.

Third, because the solids are transferred, the reactors do not have to be purged, so no purge flow is required. Actually, some steam or recycled CO_2 should be used in the reactors as sealing gas and to assist solids circulation in the loop seals. However, this flow rate is expected to be relatively small and is not taken into account in this work.

Fourth, since the CO_2/H_2O stream is produced at high temperature, a large amount of high pressure steam can be produced during cooling down of this stream. To produce high pressure steam also low temperature heat is required. Because this low temperature heat is limited, some adaptations were made to the plant design. The saturator outlet temperature was reduced to 123 °C because not much steam is required to avoid carbon deposition.

The temperature of the air reactor was set to 1200 °C, but the temperature of the fuel reactor is dependent on the solids conversion and the syngas inlet temperature. The syngas can be fed at 123 °C directly from the saturator outlet, at 300 °C by heating with high pressure saturated water or at 600 °C by feeding it to the CO_2/H_2O-cooler. The effect of the fuel feed temperature on the temperature of the fuel reactor is shown in Fig. 12. It is shown that the fuel reactor temperature is always around 1200 °C. In the previous section it was discussed that the higher the fuel feeding temperature, the higher the process efficiency. When the syngas is fed at 600 °C, the temperature in the fuel reactor is above the limit of 1200 °C. Therefore a syngas feeding temperature of 300 °C is selected, leading to an almost isothermal reactor system.

The pressure drop is assumed to be the same as for the packed bed case (5%). This depends on the solids inventory in the reactors, the reactor cross section and the pressure drop in the cyclones and the distribution plate. As was shown in Section 3.2, the effect of the pressure drop on the process efficiency is quite small, when kept below about 8%.

In case NiO is used as oxygen carrier, the conversion of the fuel is limited by thermodynamics. In that case, the selectivity of CO oxidation is 0.970 and the selectivity of H_2 oxidation is 0.985. It is assumed that the remaining CO and H_2 is combusted downstream with a stoichiometric amount of O_2 produced in the ASU (with 95% purity). The temperature of the CO_2/H_2O stream after combustion with O_2 is 1295 °C. All these assumptions lead to a mass balance as shown in Table 3. In this table, streams related to the gasification island are not included, since they do not differ from the plant with

packed bed CLC reactors. The net efficiency of this process is 41.73% of LHV. More details about the energy balance are given in Section 5.

Contrary to the packed bed configuration, the performance and behavior of the fluidized bed reactors has not been modeled in detail. Ideal assumptions have been considered, not considering some effects that might reduce the process efficiency. First of all, it is assumed that the gases are always converted as much as thermodynamically possible, which is achievable with a proper inventory, gas residence time and ΔX_s. Second, in circulating fluidized beds, also some CO_2 leakage could occur from the fuel reactor to the air reactor and some N_2 might be transported in the other direction (CO_2 dilution) (Abad et al., 2006). Also these effects, which could be minimized by utilizing small flow rates of steam as sealing gas, are not taken into account.

5. Comparison packed bed and fluidized bed

In the previous sections, the process efficiency for CLC with packed beds and circulating fluidized beds has been determined. In case of the packed bed system, the reduction could be carried out at lower temperatures. Therefore, the CO_2/H_2O stream was produced at a lower temperature (832 °C), but a large steam flow had to be mixed to reach the thermodynamic equilibrium to prevent carbon deposition at 450 °C and higher temperatures. This has a large impact on the process efficiency, because in case an oxygen carrier is selected with minimal activity for the Boudouard reaction, a smaller amount of steam is sufficient and then the process efficiency increases from 41.05% to 42.23% of LHV.

In case of the interconnected fluidized bed system, syngas dilution to avoid carbon deposition is not necessary. On the other hand, the fuel reactor operates at higher temperature and a higher fraction of the thermal input is hence available in the fuel reactor off-gas, which is recovered by raising steam. Therefore, a lower portion of heat is converted by the high temperature and high efficiency gas turbine based combined cycle. In addition, the selected oxygen carrier influences the process performance, especially if it introduces fuel conversion limitations. As a matter of fact, one of the sources of efficiency penalty in this plant is the incomplete fuel conversion due to thermodynamic limitations entailed by using Ni as oxygen carrier. In case an oxygen carrier allowing complete syngas oxidation is selected instead of NiO, the efficiency could be increased by 0.4% points, from 41.37 to 41.78%.

The energy balances of the assessed cases are reported in Table 4. The results of the packed bed and the fluidized bed Ni-based plants are reported in the third and the fourth column. The different power share of the two cases is evident, with the packed bed case generating more electricity through the gas turbine (55% of the gross power) and less by the heat recovery steam cycle (45%). This is related to the fact that CO_2 and H_2O are produced at lower temperature. In this comparison, a higher portion of the gross power (about 53%) is produced by the steam cycle in the fluidized bed case. Mainly due to the loss associated with steam dilution in the packed bed case, the process efficiency is higher in the fluidized bed case by about 0.4% points.

Moreover, two ideal cases have been compared with ideal oxygen carriers (fifth and sixth column in Table 4). Ideal means that in the packed bed case, a H_2O/CO-ratio of 0.37 is sufficient to avoid a large extent of carbon deposition (i.e. with no further steam dilution after the saturator). In the fluidized beds, the ideal OC allows full conversion of the fuel. As a consequence of these improvements, net efficiency improves by 1.1% and 0.4% points in packed bed and fluidized bed cases respectively. In this scenario, the ideal packed bed case is slightly (0.4% point) more efficient than the ideal fluidized bed case.

As far as CO_2 emissions are concerned, CLC-based plants allow a very high CO_2 capture rate, since the CO_2 is lost only from the lock hopper-based coal feeding system and from syngas combustion for coal drying. Additional CO_2 losses would occur from the CO_2 purification section if the 96.7% purity achieved were not sufficient for the storage site and the transport infrastructure.

The chemical-looping cases are compared with an IGCC power plant without CO_2 capture (first column), characterized by a net efficiency of 45.2% (Spallina et al., 2014). The CO_2 avoided and the specific primary energy consumptions for CO_2 avoided (SPECCA) is calculated with this as reference case by Eqs. (12) and (13). It is also demonstrated that with all the CLC configurations the conventional capture with Selexol (second column) is outperformed by 6–7% points.

$$CO_{2,\text{avoided}} = 1 - \frac{E_{CO_2}}{E_{CO_2,\text{ref}}} \tag{12}$$

$$\text{SPECCA} = \frac{(1/\eta_{el}) - (1/\eta_{el,\text{ref}})}{E_{CO_2} - E_{CO_2,\text{ref}}} 3600 \tag{13}$$

Table 4
Energy balances of the different cases considered for the packed bed and the fluidized bed.

Power	IGCC-NC N/A (Spallina et al., 2014)	IGCC-Sel Selexol® (Spallina et al., 2014)	PB with NiO	FzB with NiO	Ideal PB, no steam added	Ideal FzB, full gas conversion
Heat input LHV, MW_{LHV}	812.5	898.8	853.9	853.9	853.9	853.9
Gas turbine, MW_e	261.6	263.9	225.1[a]	192.1	232.2[a]	197.9
Heat Recovery Steam Cycle, MW_e	179.5	161.2	183.0	220.0	185.7	216.3
Gross power output, MW_e	441.1	425.1	408.1	412.1	417.9	414.2
Syngas blower, MW_e	−1.0	−1.1	−0.8	−0.8	−0.8	−0.8
N_2 compressor, MW_e	−34.1	−29.8				
ASU, MW_e	−29.6	−32.7	−33.9	−35.1	−33.9	−33.9
Lock hoppers CO_2 compressor, MW_e			−3.1	−3.1	−3.1	−3.1
Acid Gas Removal, MW_e	−0.4	−14.7	−0.4	−0.4	−0.4	−0.4
CO_2 compressor, MW_e		−19.7	−11.0	−11.0	−11.0	−11.0
N_2 intercooled compressor gasifier, MW_e			−1.3	−1.3	−1.3	−1.3
Heat of rejection, MW_e	−5.5	−6.3	−3.6	−3.7	−3.4	−3.6
Other auxiliaries, BOP, MW_e	−3.2	−3.6	−3.4	−3.4	−3.4	−3.4
Net power generated, MW_e	367.4	317.3	350.6	353.3	360.6	356.7
LHV efficiency, %	45.21	35.31	41.05	41.37	42.23	41.78
CO_2 capture efficiency, %		93.0	97.1	97.1	97.1	97.1
CO_2 purity, %		98.2	96.7	96.6	96.7	96.7
CO_2 emission, kg CO_2 emitted/MWh_e	769.8	101.4	24.7	24.5	24.0	24.3
CO_2 avoided, %	0	86.8	96.8	96.8	96.9	96.8
SPECCA, MJ LHV/kg CO_2		3.34	1.08	0.99	0.75	0.88

[a] Gas turbine power includes consumption of air blower and nitrogen compressor for purge.

Because the process efficiency does not depend significantly on the reactor type in which CLC is carried out, it is not expected that the process efficiency is a decisive factor in the reactor type selection. Before the reactor types could be implemented in practice, a critical unit has to be developed for high temperature/pressure application. For the packed beds, the most challenging part is probably represented by the high temperature valve system, while for the fluidized bed, hot gas filtering, loop seals and control system allowing for stable solids circulation at high pressure need to be developed. The level of development achievable for these units, their availability, operability and cost will most likely determine which technology should be used to carry out CLC integrated with the IGCC power plant.

6. Conclusions

The influence of the CLC reactor type (packed beds vs. fluidized beds) on the process efficiency has been studied. Syngas is produced in the Shell gasifier and after low temperature gas cleanup it is fed in the CLC reactors operated with NiO/Al_2O_3 oxygen carrier, which are operated at 20 bar, 1200 °C. It has been shown that for both reactor types a process efficiency (LHV basis) around 42% can be achieved.

The packed beds have the advantage that the reduction can be carried out at lower temperatures and therefore the CO_2 is produced at lower temperature. Hence, more heat is available to the gas turbine. The drawback is that more steam is required to avoid carbon deposition thereby reducing the efficiency. In case an oxygen carrier featuring slow kinetics for the Boudouard reaction is used, no additional steam has to be fed if the H_2O/CO-ratio of 0.37 reached with the saturator is assumed to be sufficient. In that ideal case, the process efficiency is increased by 1.18% points to 42.23% of LHV. So, the kinetics of the Boudouard reaction are an important factor for the oxygen carrier selection.

In the fluidized bed cases, the temperature of the CO_2/H_2O-stream is higher and this leads to a lower process efficiency. In addition, because NiO was selected as oxygen carrier, the gas conversion is relatively low and some additional oxygen was fed to reach full conversion of the gases. In the end, an LHV efficiency of 41.37% is reached. In case of a different oxygen carrier with which full gas conversion can be achieved, an LHV efficiency of 41.78% can be reached. For the circulating fluidized beds, ideal reactors were assumed (with gas conversion that follows the thermodynamics and no gas leakages) which requires proper CLC reactor system design.

From these results, it can be concluded that the selection of the reactor type does not have a large influence on the process efficiency. In the packed bed case, a high temperature valve system needs to be designed, while for the fluidized beds, high temperature filtering and a solid circulation control system have to be developed, which seems to be a much bigger challenge compared to a valve system. The development, operability and costs of these parts will determine which type of reactor is more suitable for large scale CLC application.

Acknowledgement

The research originating these results has been supported by the CATO-2 program under the project number WP1.3F2.

References

Abad, A., Mattisson, T., Lyngfelt, A., Ryden, M., 2006. Chemical-looping combustion in a 300 W continuously operating reactor system using a manganese-based oxygen carrier. Fuel 85, 1174–1185.

Abad, A., Adánez, J., García-Labiano, F., de Diego, L.F., Gayán, P., Celaya, J., 2007. Mapping of the range of operational conditions for Cu-, Fe-, and Ni-based oxygen carriers in chemical-looping combustion. Chem. Eng. Sci. 62, 533–549.

Adanez, J., Abad, A., Garcia-Labiano, F., Gayan, P., de Diego, L.F., 2012. Progress in chemical-looping combustion and reforming technologies. Prog. Energy Combust. Sci. 38, 215–282.

Anantharaman, R., Bolland, O., Booth, N., van Dorst, E., Ekstrom, C., Sanchez Fernandes, E., Franco, F., Macchi, E., Manzolini, G., Nikolic, D., et al., 2011. European best practice guidelines for assessment of CO_2 capture technologies., pp. 99, www.gecos.polimi.it/research/EBTF_best_practice_guide.pdf

Barin, I., 1993. Thermochemical Data of Pure Substances. VCH, Weinheim.

Chiesa, P., Macchi, E., 2004. A thermodynamic analysis of different options to break 60% electric efficiency in combined cycle power plants. ASME J. Eng. Gas Turbines Power 126, 770–785.

Consonni, S., Lozza, G., Pelliccia, G., Rossini, S., Saviano, F., 2006. Chemical-looping combustion for combined cycles with CO_2 capture. ASME J. Eng. Gas Turbines Power 128, 525.

Ergun, S., 1952. Fluid flow through packed columns. Chem. Eng. Prog. 48, 89–94.

Erlach, B., Schmidt, M., Tsatsaronis, G., 2011. Comparison of carbon capture IGCC with pre-combustion decarbonisation and with chemical-looping combustion. Energy 36, 3804–3815.

GECOS, 2013. GS software, www.gecos.polimi.it/software/gs.php

Håkonsen, S.F., Blom, R., 2011. Chemical looping combustion in a rotating bed reactor – finding optimal process conditions for prototype reactor. Environ. Sci. Technol. 45, 9619–9626.

Håkonsen, S.F., Grande, C.A., Blom, R., 2014. Rotating bed reactor for CLC: bed characteristics dependencies on internal gas mixing. Appl. Energy 113, 1952–1957.

Hamers, H.P., Gallucci, F., Cobden, P.D., Kimball, E., van Sint Annaland, M., 2013. A novel reactor configuration for packed bed chemical-looping combustion of syngas. Int. J. Greenh. Gas Control 16, 1–12.

IEA, 2005. Oxy combustion processes for CO_2 capture from power plant, report 2005/9.

IPCC, 2013. Climate Change 2013: The Physical Science Basis. In: Stocker, T.F., Qin, D., Plattner, G.-K., Tignor, M., Allen, S.K., Boschung, J., Nauels, A., Xia, Y., Bex, V., Midgley, P.M. (Eds.), Contribution of Working Group I to the Fifth Assessment Report of the Intergovernmental Panel on Climate Change. Cambridge University Press, Cambridge, United Kingdom and New York, NY, USA, p. 1535.

Jerndal, E., Mattisson, T., Lyngfelt, A., 2006. Thermal analysis of chemical-looping combustion. Chem. Eng. Res. Des. 84, 795–806.

Kjelstrup, S., Hustad, J.E., Gundersen, T., Lior, N., Naqvi, R., Wolf, J., Bolland, O., 2007. Part-load analysis of a chemical looping combustion (CLC) combined cycle with CO_2 capture. Energy 32, 360–370.

Kolbitsch, P., Pröll, T., Bolhar-Nordenkampf, J., Hofbauer, H., 2009. Characterization of chemical looping pilot plant performance via experimental determination of solids conversion. Energy Fuels 23, 1450–1455.

Kolbitsch, P., Bolhàr-Nordenkampf, J., Pröll, T., Hofbauer, H., 2010. Operating experience with chemical looping combustion in a 120 kW dual circulating fluidized bed (DCFB) unit. Int. J. Greenh. Gas Control 4, 180–185.

Lyngfelt, A., 2014. Chemical-looping combustion of solid fuels – status of development. Appl. Energy 113, 1869–1873.

Mattisson, T., García-Labiano, F., Kronberger, B., Lyngfelt, A., Adánez, J., Hofbauer, H., 2007. Chemical-looping combustion using syngas as fuel. Int. J. Greenh. Gas Control 1, 158–169.

Mattisson, T., Lyngfelt, A., Leion, H., 2009. Chemical-looping with oxygen uncoupling for combustion of solid fuels. Int. J. Greenh. Gas Control 3, 11–19.

Moldenhauer, P., Rydén, M., Mattisson, T., Younes, M., Lyngfelt, A., 2014. The use of ilmenite as oxygen carrier with kerosene in a 300 W CLC laboratory reactor with continuous circulation. Appl. Energy 113, 1846–1854.

Naqvi, R., Bolland, O., 2007. Multi-stage chemical looping combustion (CLC) for combined cycles with CO_2 capture. Int. J. Greenh. Gas Control 1, 19–30.

Natesan, K., Zeng, Z., 2003. Study of metal dusting phenomenon and development of material resistant to metal dusting. final report for DOE. ANL-03/33.

Noorman, S., van Sint Annaland, M., Kuipers, 2007. Packed bed reactor technology for chemical-looping combustion. ACS Ind. Eng. Chem. Res. 46, 4212–4220.

Noorman, S., van Sint Annaland, M., Kuipers, J.A.M., 2010. Experimental validation of packed bed chemical-looping combustion. Chem. Eng. Sci. 65, 92–97.

Rezvani, S., Huang, Y., McIlveen-Wright, D., Hewitt, N., Mondol, J.D., 2009. Comparative assessment of coal fired IGCC systems with CO_2 capture using physical absorption, membrane reactors and chemical looping. Fuel 88, 2463–2472.

Schmidt, E., 1982. Properties of Water and Steam in SI Units. Springer-Verlag, Berlin.

Seider, W.D., Seader, J.D., Lewin, D.R., 2004. Cost accounting and capital cost estimation (chapter 16). In: Product & Process Design Principles (second edition). John Wiley and Sons, Inc., New York, NY, USA, pp. 473–562.

Sinnott, R.K., 2005. Chemical engineering design, section 13.5. In: Chemical Engineering Design (fourth edition). Elsevier, Oxford, United Kingdom, pp. 815.

Spallina, V., Gallucci, F., Romano, M.C., Chiesa, P., Lozza, G., van Sint Annaland, M., 2013. Investigation of heat management for CLC of syngas in packed bed reactors. Chem. Eng. J. 225, 174–191.

Spallina, V., Romano, M.C., Chiesa, P., Gallucci, F., van Sint Annaland, M., Lozza, G., Hamers, H.P., Romano, M.C., Spallina, V., Chiesa, P., et al., 2014. Integration of coal gasification and packed bed CLC process for high efficiency and near-zero emission power generation. Int. J. Greenh. Gas Control 27, 28–41.

ThermalCeramics, 2013. JM23 saving you energy brochure, http://www.morganthermalceramics.com/products/insulating-fire-bricks-ifb/
Wolf, J., Anheden, M., Yan, J., 2005. Comparison of nickel- and iron-based oxygen carriers in chemical looping combustion for CO_2 capture in power generation. Fuel 84, 993–1006.
2014. World steel prices, http://www.worldsteelprices.com
Zaabout, A., Cloete, S., Johansen, S.T., van Sint Annaland, M., Gallucci, F., Amini, S., 2013. Experimental demonstration of a novel gas switching combustion reactor for power production with integrated CO_2 capture. ACS Ind. Eng. Chem. Res. 52, 14241–14250.